



Exergetic and economic comparison of ORC and Kalina cycle for low temperature enhanced geothermal system in Brazil



Carlos Eymel Campos Rodríguez^{a,*}, José Carlos Escobar Palacio^a, Osvaldo J. Venturini^a,
Electo E. Silva Lora^a, Vladimir Melián Cobas^a, Daniel Marques dos Santos^b,
Fábio R. Lofrano Dotto^c, Vernei Gialluca^d

^a Federal University of Itajuba (UNIFEI), Mechanical Engineering Institute – IEM, Excellence Group in Thermal Power and Distributed Generation (NEST), Minas Gerais, Brazil

^b AES Tietê, Bauru, São Paulo, Brazil

^c FAROL Pesquisa, Desenvolvimento e Consultoria, Brazil

^d Gênera Serviços e Comércio LTDA, Brazil

HIGHLIGHTS

- The aim of this paper is to compare both cycles (ORC and Kalina).
- Kalina cycle offer 18% more net power than ORC and require 37% less mass flow rate.
- It was obtained 17.8% lower levelized electricity costs for Kalina cycle over the ORC.

ARTICLE INFO

Article history:

Received 1 August 2012

Accepted 7 November 2012

Available online 24 November 2012

Keywords:

Thermodynamic analysis
Kalina cycle
Organic Rankine cycle
Enhanced geothermal system
Working fluids
Ammonia–water mixture
Exergy
Levelized electricity cost

ABSTRACT

This paper deals with the thermodynamic analysis, of both the first and second law of thermodynamic of two different technologies, (ORC and Kalina cycle) for power production through an enhanced geothermal system (EGS). In order to find a better performance of both thermal cycles it were evaluated 15 different working fluids for ORC and three different composition of the ammonia–water mixture for the Kalina cycle. In this work, the Aspen-HYSYS software was used to simulate both thermal cycles and to calculate the thermodynamic properties based on Peng–Robinson Stryjek–Vera (PRSV) Equation of State (EoS). At the end the two cycles was compared using an economic analysis with the fluid that offers the best performance for each thermal cycle which are R-290 for ORC and for Kalina cycle a composition of the mixture of 84% of ammonia mass fraction and 16% of water mass fraction. For this conditions the Kalina cycle produce 18% more net power than the ORC. A levelized electricity costs of 0.22 €/kW h was reached for ORC and 0.18 €/kW h for Kalina cycle. Finally a sensitivity analysis of the EGS LCOE was carried out for a few economic parameters to determinate how is the variation of LCOE for a % change from the base case.

© 2012 Elsevier Ltd. All rights reserved.

1. Introduction

World energy demand is expected to continue to increase in a foreseen future. In order to minimize the negative impact on environment caused by utilization of fossil energy resources, more efficient energy conversion processes and the use of “clean energy” are necessary. The electrical power demand is also expected to increase. The fact that most of our energy supply comes from carbon-based

sources, increase the concentration of carbon dioxide and other greenhouse gases in the atmosphere. In addition, the emissions of methane, nitrous oxide, and other halocarbons increase too.

Geothermal energy is based on the heat from the Earth. It's clean and sustainable. Resources of geothermal energy range from the shallow ground to hot water and hot rock found a few miles beneath the Earth's surface, and down even deeper to the extremely high temperatures of molten rock called magma. The Earth's geothermal resources are theoretically more than enough to supply humanity's energy needs [1,2].

The Brazilian energetic matrix is based mainly in renewable sources (about 80% hydro and 6% biomass and wind). The application of the geothermal heat in Brazil is limited to it direct use only. The various applications of direct use are: 0.9 MWt and

* Corresponding author.

E-mail addresses: eymelcampos@hotmail.com (C.E. Campos Rodríguez), danielmarques.santos@aes.com (D. Marques dos Santos), fabio@farolconsultoria.com.br (F.R. Lofrano Dotto), vernei@generatech.com.br (V. Gialluca).

Nomenclature

P	pressure, (kPa)
T	(absolute) temperature, (K)
t	temperature, ($^{\circ}\text{C}$)
R	gas constant, (J/kg K)
V	specific volume, (m^3/kg)
w	acentric factor of the working fluid
a, b	parameters of the state equation
\bar{U}	global heat transfer coefficient, ($\text{W}/\text{m}^2 \text{ K}$)
A	area (m^2)
\dot{m}	mass flow rate (kg/s)
\dot{Q}	heat rate (kW)
\dot{W}	power rate (kW)
h	enthalpy (kJ/kg)
e	specific exergy (kJ/kg)
s	entropy (kJ/kg K)
\dot{E}	exergy (kW)
η	efficiency (%)
q	total heat transfer

Subscripts

c	critical
r	reduced temperature ($T_r = T/T_c$)
in	inlet
out	outlet
0	dead state
t	turbine
p	pump
d	destruction
w	geothermal fluid
th	thermal
e	exergy
eq	equipment
h	hot
c	cold

Abbreviations

HT	high temperature
LT	low temperature
LCOE	levelized electricity costs

15.4 TJ/yr for fish farming, 4.20 MWt and 77.0 TJ/yr for an industrial wool processing plant; 355 MWt and 6530 TJ/yr for bathing and swimming, for a total of 360.1 MWt and 6622.4 TJ/yr [35]. A significant number of low temperature resources ($<90^{\circ}\text{C}$) have been identified in the continental area, but the potential for high temperature geothermal systems appears to be restricted to the Atlantic islands of Fernando de Noronha and Trindade. Most of the springs that account for the potential are located in the west central Brazil (in the states of Goiás and Mato Grosso) and in the south (in the state of Santa Catarina) [14].

For low-grade geothermal reservoir with a temperature of 150°C or lower, the common type of power plant to build is a binary plant. This kind of plant use as working fluid, organic fluids (ORC) or ammonia–water mixture (Kalina cycle), both with low boiling points to recover heat from low-temperature heat source. Today, binary plants are the most widely used type of geothermal power plant with 162 units in operation, generating 373 MW of power in 17 countries, and making up to 32% of all geothermal units, but only 4% of the total power [1].

In a binary cycle power plant the heat of the geothermal water is transferred to a secondary working fluid, usually an organic fluid or a mixture, that has a lower boiling point and high vapor pressure compared to water at a given temperature. This type of geothermal plant has no emissions to the atmosphere. Thus, environmental problems that may be associated with the exploitation of higher temperature geothermal resources, like the release of greenhouse gases and the discharge of toxic elements, are avoided. Another advantage of the binary technology is that the geothermal fluids (or brines) do not contact the moving mechanical components of the plant (like turbine), assuring a longer life for the equipment. Binary plants have allowed the exploitation of a large number of fields that may have been very difficult (or uneconomic) when using other energy conversion technologies, thereby increasing significantly the development of geothermal resources worldwide.

For low-temperature geothermal systems that only produce hot water, geothermal binary power plants show very low values of First law efficiencies (5–12%); even Second law efficiencies are typically in the 25–50% range [3–8]. In recent years there have

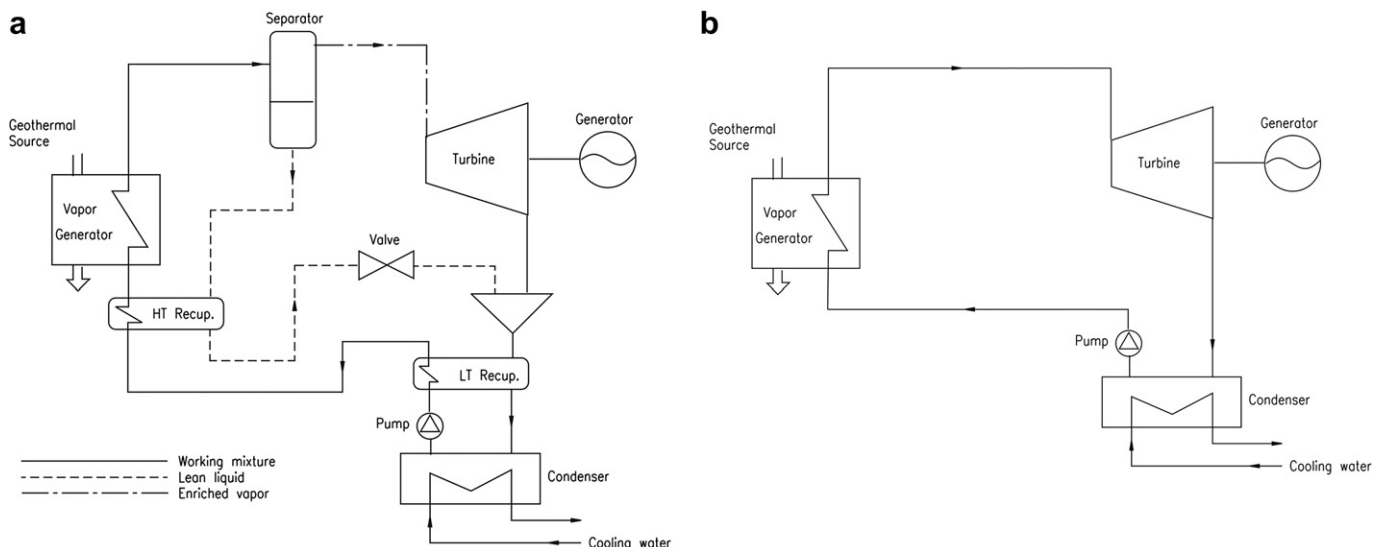


Fig. 1. Schematic components layout in a geothermal power plant. a) Kalina cycle and b) ORC.

Table 1
Thermodynamic parameters of the considered pure working fluids.

Working fluids	T_c (°C)	P_c (kPa)	T_b (°C)	M (Kg/Kmol)	ω	k_1	Type
<i>n</i> -Pentane	196.45	3375	36.06	72.15	0.25389	0.02227	Dry
<i>i</i> -Pentane	187.25	3334	27.88	72.15	0.22222	0.04451	Dry
<i>n</i> -Butane	152.05	3797	−0.5	58.12	0.2010	0.03951	Dry
<i>i</i> -Butane	134.95	3648	−11.73	58.12	0.18479	0.03781	Dry
R134a	100.99	4055	−26.22	102.03	0.3256	0.07076	Isentropic
R141b	116.95	4340	31.99	116.95	0.2211	0.05949	Isentropic
R142b	137.05	4120	−10.01	100.5	0.2360	0.00689	Isentropic
R290	96.66	4242	−42.08	44.10	0.1488	0.19724	Isentropic
R40	143.15	6700	−24.05	50.49	0.1530	0.03040	Wet
R152a	113.89	4444	−25	66.05	0.2557	−0.14590	Isentropic
R-11	198.05	4408	22.9	137.37	0.1910	0.02574	Isentropic
R-12	111.85	4124	−29.75	120.91	0.1760	0.02752	Isentropic
R-113	214.1	3436	47.57	187.39	0.245	−0.02468	Dry
R-114	145.89	3621	3.68	170.92	0.2502	0.05823	Dry
R-21	178.43	5184	8.9	102.92	0.2069	0.03808	Isentropic
NH ₃	133.7	11600	−249.85	17	0.2526	−0.2432	Wet
H ₂ O	374.2	22100	373.15	18	0.3449	1.7999	Wet

been many studies that have attempted to increase binary plant efficiencies; they focused mainly on the combination of the working fluid [9–12].

The selection of the working fluids for ORC system (Fig. 1b) has been well discussed by many authors [13–17]. These fluids properties have a direct influence over the cycle, such as: thermal conductivity, the slope of the T – s curve, critical temperature and pressure, molecular mass, density, latent heat, etc.

Kalina cycle, using ammonia–water as working fluid (Fig. 1a) is conceptually different from the Rankine cycles working with non-azeotropic mixtures, even though its final thermodynamic aim is the same: the reduction of thermal irreversibilities obtained. Recent publications [10,12,18], show efficiency advantages for Kalina cycle over ORCs, due to, mainly, its non-constant evaporation temperature in a transition from saturated liquid to saturated vapor.

2. Technologies description and simulation

The main difference between the two technologies is that Kalina cycle use an ammonia–water mixture as working fluids while the ORC working fluid is a pure organic fluid. The utilization of a mixture as a working fluid is to take advantage of the non-constant evaporation temperature in order to reduce entropy generation and achieve a higher specific work potential.

An ORC system using low-grade energy sources is depicted in Fig. 1b. The system is composed by an evaporator, a turbine expander, a condenser, and a pump. The working fluid passes through the evaporator in which the high-temperature geothermal

source is utilized. The vapor enters the turbine expander and generates power. The fluid exit from the turbine expander then enters the condenser in which low-temperature cooling water is utilized to condense the fluid. Finally, a pump raises fluid pressure and feeds the fluid into the evaporator to complete the cycle.

The process flow diagram of Kalina cycle is given in Fig. 1a. The main components of the Kalina cycle plant are: evaporator, separators, low and high temperature recuperator, circulation pump, condenser and turbine-generator. The ammonia–water mixture is heated in the high-temperature recuperator and evaporator; ammonia-rich vapor is separated in the separator and sent to the turbine-generator. After passing through the turbine-generator, the expanded ammonia-rich liquid is mixed in the low-temperature recuperator with the cool ammonia-poor liquid from the separator and sent to the condenser, whence it is recirculated to the evaporator to complete the cycle.

The performance of the two technologies is compared in this study under identical conditions of the enhanced geothermal system, in order to reach a maximum specific work and efficiency. We assume a relative simple configuration for Kalina cycle (scheme similar to the Húsavík plant [19]) because the low-temperature of the geothermal source and the limited power level do not justify an excessive plant scheme complication. The configuration of the considered ORC is subcritical cycles with saturated vapor at the turbine inlet (for both technologies) in order to achieve the maximum power output and efficiency, due to superheat contributes negatively to the cycle efficiency for dry and isentropic fluids, and is not recommended [8,14].

3. Calculation model

The thermodynamic analysis of the considered cycles was carried out by using the commercial software Aspen-HYSYS and cubic equation of state Peng–Robinson Stryjek–Vera [20] for the working fluids thermodynamic properties calculation (1–6).

$$P = \frac{RT}{v-b} - \frac{a}{v(v+b) + b(v-b)} \quad (1)$$

Where

$$a = (\alpha)0.45724 \frac{R^2 T_c^2}{P_{cr}} \quad (2)$$

$$\alpha = \left[1 + k \left(1 - T_r^{0.5} \right) \right]^2 \quad (3)$$

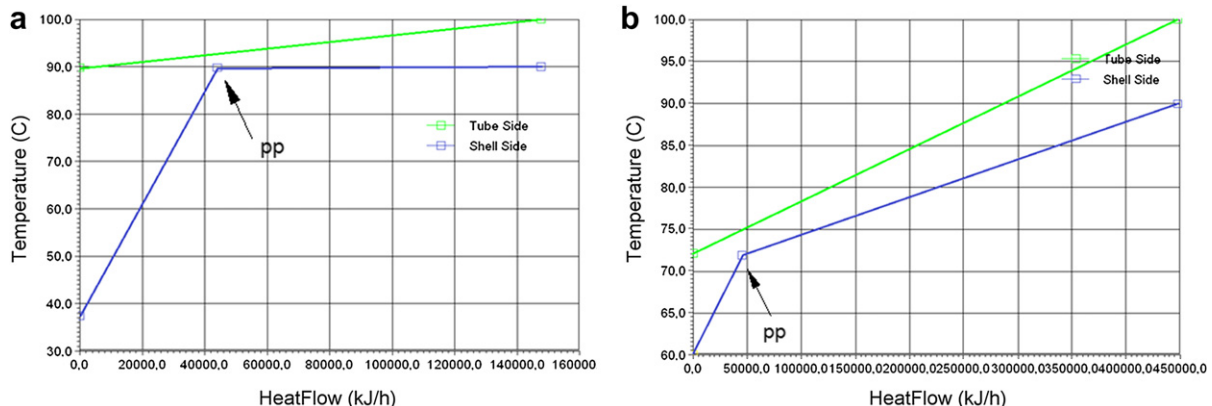


Fig. 2. Pinch point (pp) at the evaporation process. a) ORC and b) Kalina cycle.

$$b = 0.0777896 \frac{RT_c}{P_c} \quad (4)$$

$$k = k_0 + k_1 (1 + T_r^{0.5}) (0.7 - T_r) \quad (5)$$

$$k_0 = 0.378893 + 1.489715\omega - 0.1713848\omega^2 + 0.0196544\omega^3 \quad (6)$$

and k_1 is the single pure compound adjustable parameter and is dependent on the values used for the critical constants T_c and P_c and for the acentric factor ω .

In this paper, we consider 15 pure substances as working fluids for ORC and 3 different concentration of ammonia–water mixture (65%, 75% and 84% of ammonia mass fraction) for Kalina cycle. For each one, main thermodynamic parameters are listed in Table 1.

The aim of this paper is to compare both cycles (ORC and Kalina) in order to determinate, by mean of thermodynamic and economic criteria, which is the cycle that offer better performances for Brazilian conditions. This analysis is restricted to low temperature geothermal source (90–140 °C) and condensing temperatures of 37 °C. For this analysis it was taken as the basis of calculation 1 kg/s of the geothermal source, the pinch point (pp) was set at 3 °C at the evaporation start and the terminal temperature differential (TTD) of 10 °C between the geothermal source temperature and the evaporator outlet temperature of the working fluid, the outlet temperature of the geothermal fluid is calculated from previous assumptions, as shown in Fig. 2. This figure shows the evaporation process of the geothermal fluid temperature in ORC and Kalina cycle at 100 °C. Here is observed how Kalina cycle cause minors irreversibilities in the evaporator, due to the non-constant temperature in the evaporation process if compared with ORC. For this analysis was assumed (for ORC), a subcritical cycle without overheated vapor, in order to reach higher power output and efficiencies [21]. The isentropic efficiency of the turbine and pump was assumed 85% and 80% respectively for each system.

For low-temperature geothermal source another challenge is that the temperature level of heat extraction is low. This in turn reduces the power produced per unit of working fluid. The pinch temperature at evaporation restricts the evaporation pressure and

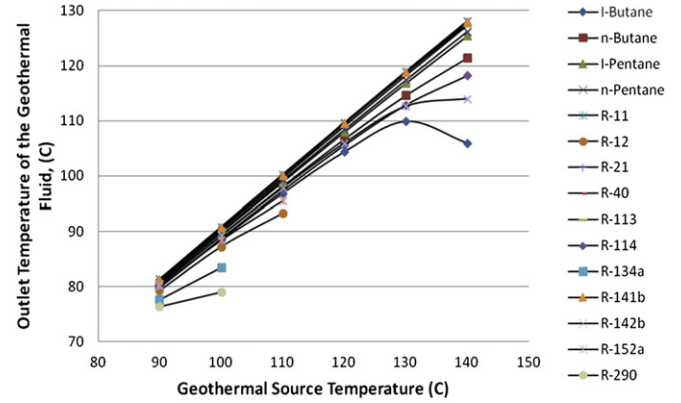


Fig. 3. Outlet temperature of the geothermal fluid for the different inlet temperatures and working fluids.

it is difficult to lower the heat source temperature to lowest possible level. As the pinch in the heat exchanger decreases, more heat is absorbed and thereby more power is produced, but the heat exchanger area will increase and the tradeoff between heat exchanger area and power production is an important fact to consider [36].

4. Energy and exergy balance for both cycles components

Mass and energy balances for each component of the thermal system can be established using Equations (7),(8), neglecting the changes in kinetic and potential energies.

$$\sum \dot{m}_{in} = \sum \dot{m}_{out} \quad (7)$$

$$\dot{Q} - \dot{W} = \sum \dot{m}_{out} h_{out} - \sum \dot{m}_{in} h_{in} \quad (8)$$

The energy balance equations for ORC and Kalina cycle components are given in Table 2 (Equations (9)–(15)).

The pinch point temperature in the evaporator was set at evaporation starts (see Fig. 2a and b), for ORC and Kalina cycle. In the condenser was assumed an increasing water temperature of 10 °C and the ambient temperature of 25 °C.

The exergy rate of geothermal fluid, working fluid and condensing water, is given by [23]:

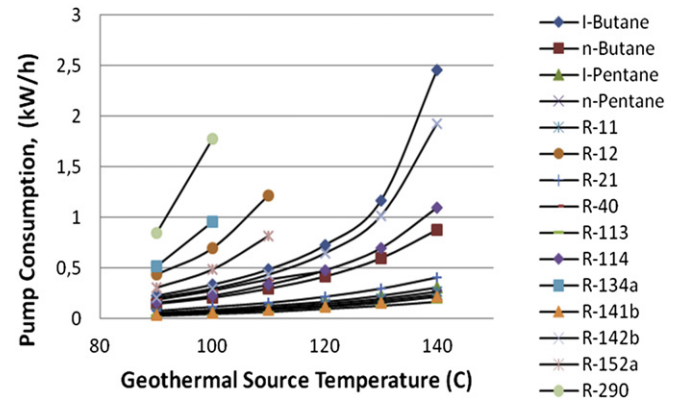


Fig. 4. Pump energy consumption for each working fluid.

Table 2
Equations for ORC and Kalina cycle components.

Components	Energy balance equations → Equations no.
Turbine	$\dot{W}_t = \dot{m}_{wf} (h_{in} - h_{out})$ (9)
Pump	$\dot{W}_p = \dot{m}_{wf} (h_{out} - h_{in})$ (10)
Evaporator	$\dot{m}_{gw} (h_{in_{gw}} - h_{out_{gw}}) = \dot{m}_{wf} (h_{out_{wf}} - h_{in_{wf}})$ (11)
Condenser	$\dot{m}_w (h_{out_w} - h_{in_w}) = \dot{m}_{wf} (h_{in_{wf}} - h_{out_{wf}})$ (12)
HT recuperator	$\dot{m}_{lf} (h_{in_{lf}} - h_{out_{lf}}) = \dot{m}_{wf} (h_{out_{wf}} - h_{in_{wf}})$ (13)
LT recuperator	$\dot{m}_{wf} (h_{in_{wf}} - h_{out_{wf}}) = \dot{m}_{wf} (h_{out_{wf}} - h_{in_{wf}})$ (14)
Generator	$\dot{W}_{net} = 0.95 \cdot \dot{W}_t$ (15)

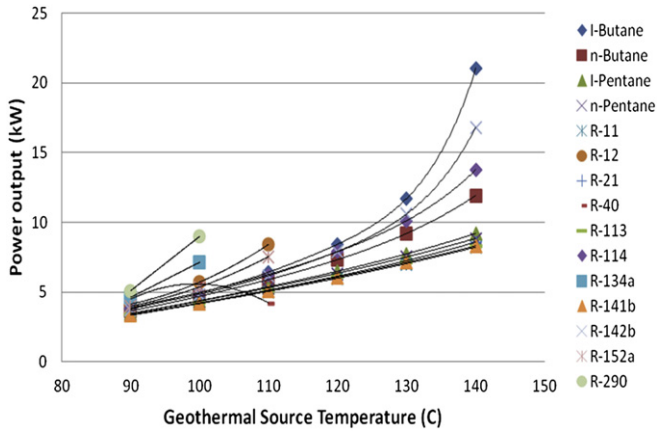


Fig. 5. Power output for 15 working fluids.

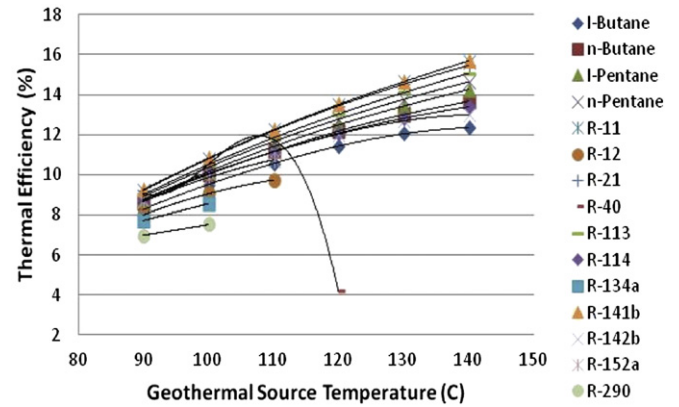


Fig. 7. Thermal efficiency for the different working fluids.

$$\dot{E} = \dot{m}[(h - h_0) - T_0(s - s_0)] \quad (16)$$

Where the properties in the dead state are evaluated at T_0 and P_0 . When the fluid is in the liquid phase at the dead-state conditions, it is sufficiently accurate to take the dead-state enthalpy and entropy values as if the fluid is a saturated liquid at the dead-state temperature, for this case, 25 °C.

The exergy destruction of each component can be found from an exergy balance.

$$\dot{E}_d = \sum \dot{E}_{out} - \sum \dot{E}_{in} - \dot{W} \quad (17)$$

The overall thermal and exergy efficiency are defined as:

$$\eta_{th} = \frac{\dot{W}_t - \dot{W}_p}{\dot{Q}_{in}} \quad (18)$$

$$\eta_{ex} = \frac{\dot{W}_t - \dot{W}_p}{\dot{E}_{out} - \dot{E}_{in}} \quad (19)$$

5. Evaluation of the organic Rankine cycle performance

As shown in Fig. 3, there is a different outlet temperature of the geothermal fluid for each working fluid. This outlet temperature

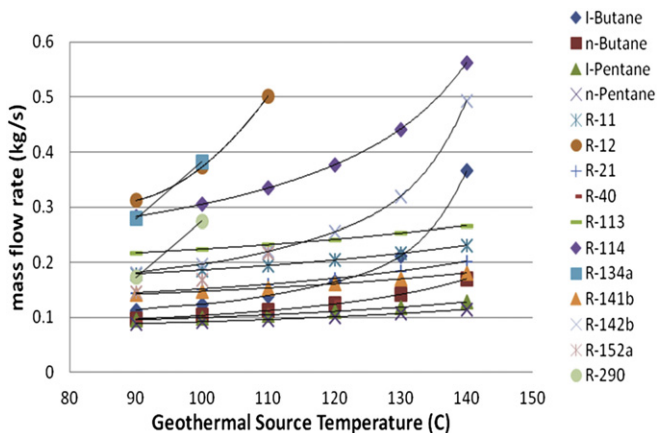


Fig. 6. Mass flow rate for the different working fluids for 1 kg/s of the geothermal source.

depends on the type of the thermal system used, the selection of the pinch point temperature and the heat absorption capacity of the working fluid. Figs. 5 and 6, show the power output reached by using different organic working fluids and the mass flow rate that is able to be evaporated. Higher power output is reached when the difference between the temperature of the geothermal source and the critical temperature of the working fluid is minimal, (evaporation pressure closer of the critical point of the working fluid). Maximum power output of 21.06 kW is reached evaporating 0.37 kg/s of I-Butane at 140 °C of the geothermal source (Fig. 4).

In Figs. 7 and 8 are shown the thermal and exergetic efficiencies of the cycle, for different working fluids and a geothermal source of 90 °C–140 °C. The thermal efficiency varies between 7 and 15.9% while the exergetic efficiency varies between 42.5 and 59%. Is important to note that fluids that hold lower Thermal and exergetic efficiency correspond to fluids that produce higher power output, which allow to evaporate a greater quantity of working fluid.

In Fig. 9 is shown the exergy destruction in each component of the cycle for the different working fluids. The exergy destruction in the cycle behaves as follow: the evaporator is responsible for the biggest irreversibility, followed by the turbine or condenser and finally the pump. In dry fluids, the second largest exergy destroyer in the cycle is the condenser, due to the fact that at the exit of the turbine expansion the fluid is in a superheated region and the temperature differential of

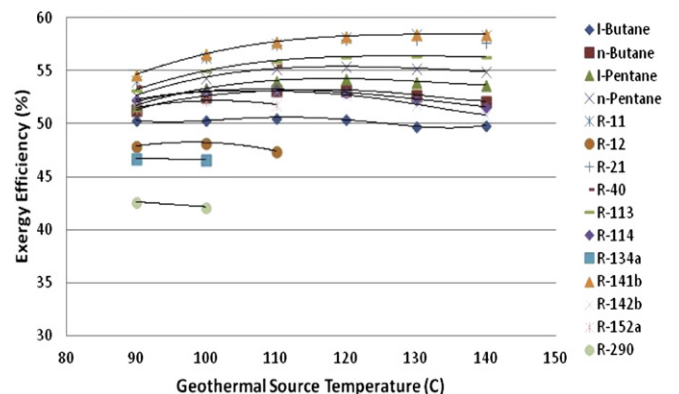


Fig. 8. Exergetic efficiency for the different working fluids.

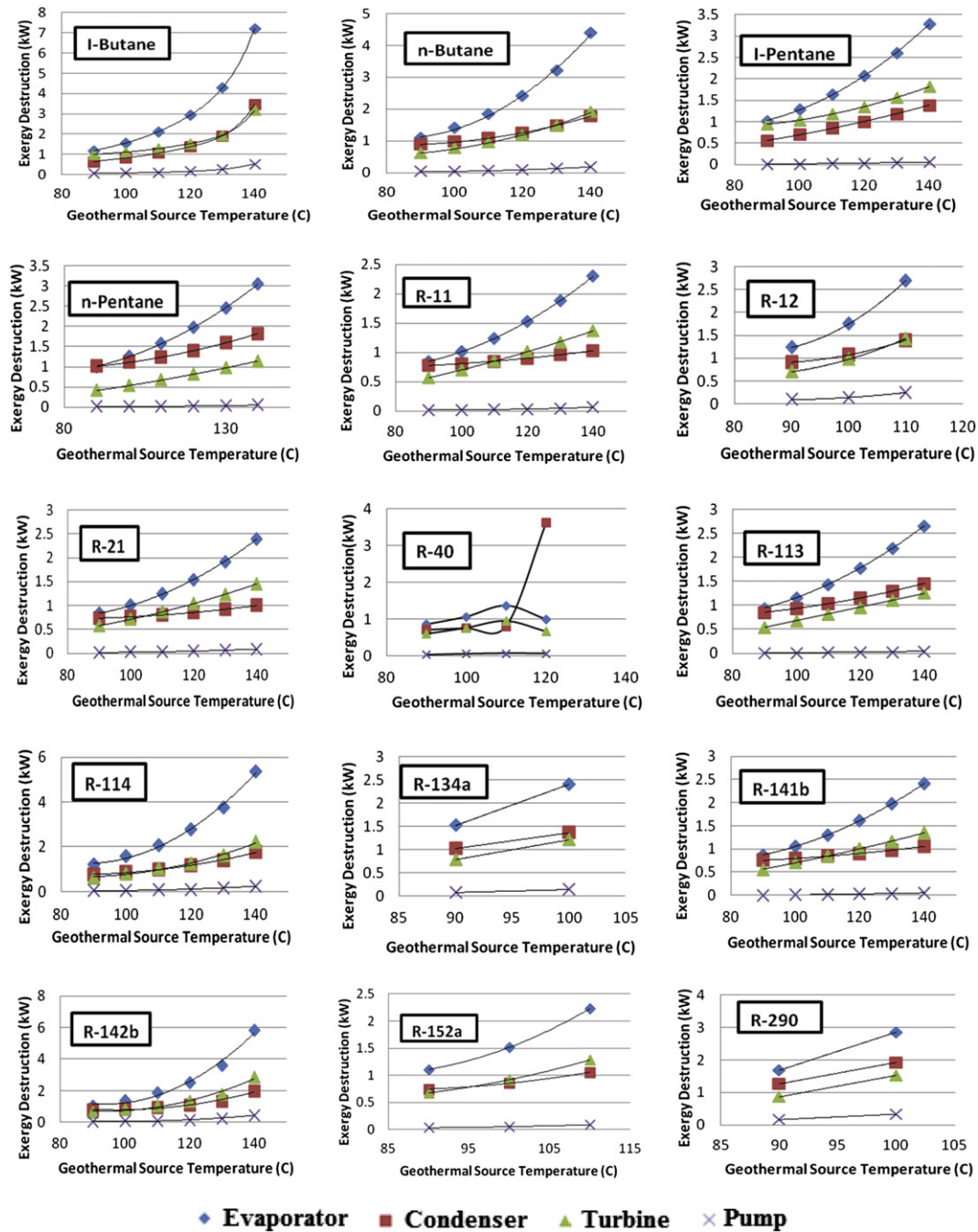


Fig. 9. Exergy destruction by components of the ORC.

the working fluid and the condensation water is higher than in wet and isentropic fluids, while, in wet fluids, as R-40, it is necessary to do a small superheating before the working fluid enter in the turbine to avoid qualities of the vapor lower than 0.9 at the end of the expansion process that can cause damages in the equipment (Fig. 10).

6. Evaluation of the Kalina cycle performance

First, the optimum working pressure was evaluated, in order to obtain a maximum power output, at saturated conditions in the turbine inlet for different compositions of the working fluid, that vary from 65%, 75% and 84% of ammonia mass fraction in

the mixture and a geothermal source temperature from 90 °C to 140 °C as shown in Fig. 11 [30]. It can be observed that the power output varies with the working pressure, temperature and composition of the ammonia–water mixture. At each concentration and temperature, we obtain a maximum power output under a determined working pressure (Figs. 12 and 13).

Figs. 14 and 15 show the power output, thermal and exergetic efficiency of the Kalina cycle working at different ammonia mass fraction. The maximum power output reached is 28.05 kW at a geothermal source of 140 °C and 84% of ammonia mass fraction. The comparison of different concentration of the working fluids in relation to the mass flow rate and the quantity of this mass that

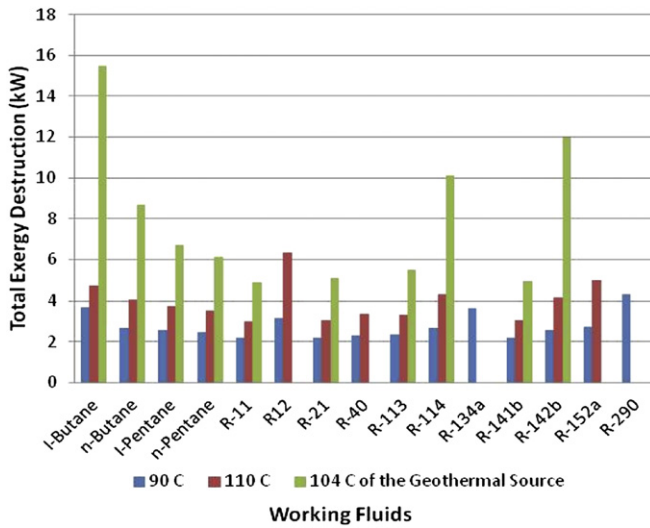


Fig. 10. Total exergy destruction for the different working fluids of the ORC.

can be evaporate in the Kalina cycle, as shown in Figs. 16 and 17 for different geothermal source temperature, can be conclude that working at 84% of ammonia mass fraction the cycle require less mass flow rate and is able to evaporate a higher part of this mass flow rate for the same geothermal heat, allowing to work with smaller equipments size and, consequently, less expensive cycles.

The exergy destruction in the components of the cycle was calculated for Kalina cycle and the results are shown in Fig. 18. The

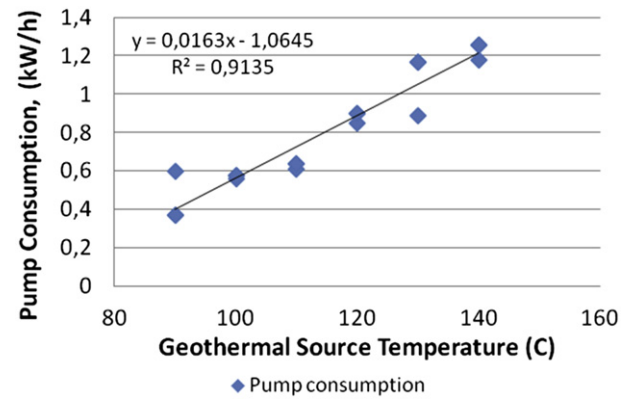


Fig. 12. Pump energy consumption for the different concentration of the ammonia–water mixture.

component responsible for higher exergy destruction is the condenser, followed by the evaporator, then turbine, HT recuperator and LT recuperator. For each case the total exergy destroyed is almost the same working at determinate geothermal source temperature (Fig. 19).

7. Economic analysis

The calculation of the LCOE is based on the estimation of the prospective costs (and revenues from possible by-products) since only one commercial plant exists so far, located at Landau in south west Germany. The prospective costs thereby depend on

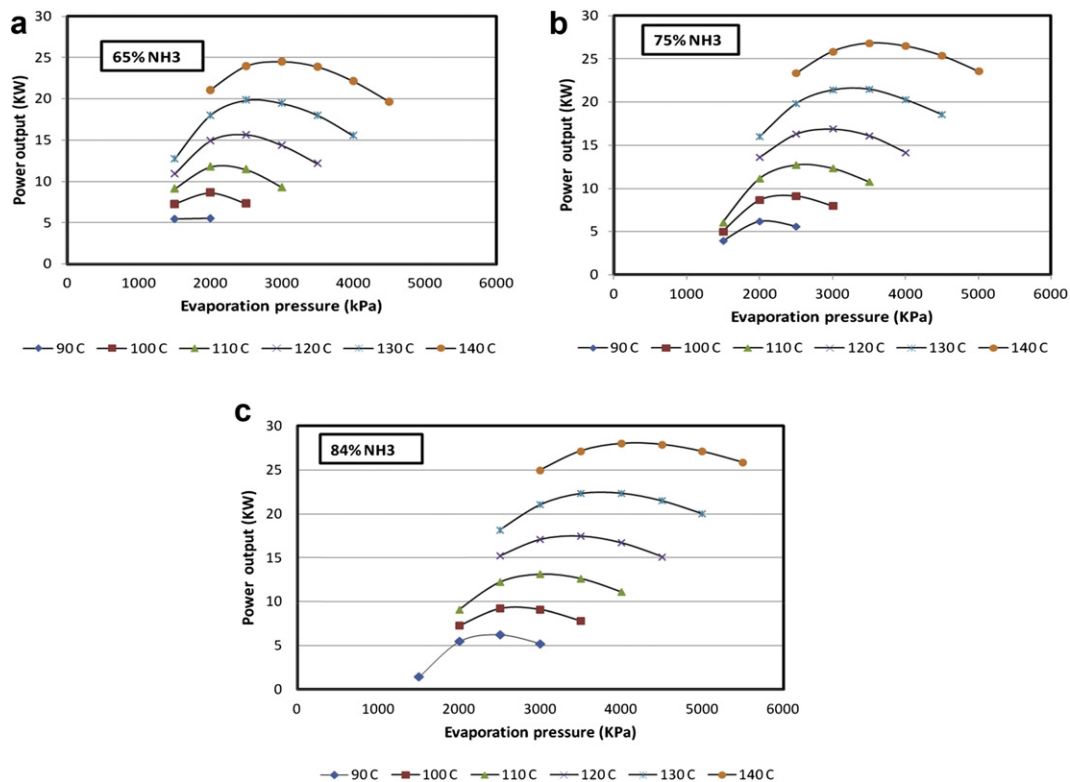


Fig. 11. Cycle maximum power achieved for different temperatures of the geothermal source and evaporation pressures. (a) 65% of ammonia fraction (b) 75% of ammonia fraction (c) 84% of ammonia fraction.

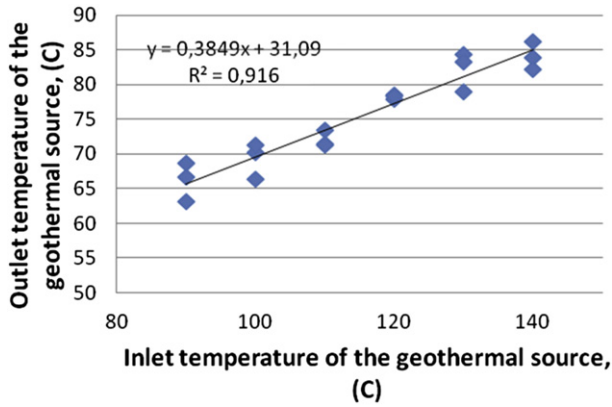


Fig. 13. Outlet temperature vs inlet temperature of the geothermal fluid for the different concentration of the ammonia–water mixture.

the site and project-specific conditions. Accordingly, LCOE, which is representative for all EGS sites, is estimated between €20 and €30 cents/kW h [34]. However, the general cost structure and influencing factors should be similar for different projects. The methodology to calculate the LCOE is a commonly applied approach that is described in detail in [2,22,31–33] and shown in Table 6. In Table 4 are shown the operational parameters for a EGS project using as energy conversion system an ORC and a Kalina cycle for Brazilian conditions [35], (100 °C and 200 kg/s of geothermal water), working with the fluid or mixture, that offer the better performance for each technology, analyzed above.

Detailed exploration and drilling cost calculations use geographical and geological site information. Such calculations usually consider also a supplemental charge for unforeseen events, such as stuck pipes or hole-stability problems. This charge typically lies between 10 and 20%, but can be higher in unknown geologic areas [24].

The size of the main components (heat exchangers, pumps and turbine) are estimated for both cycles. Basically, the size of the heat exchanger can be calculated using the LMTD methods (log Mean Temperature Difference) [25],

The total heat transfer rate per unit of time (q) can be expressed in the following equations:

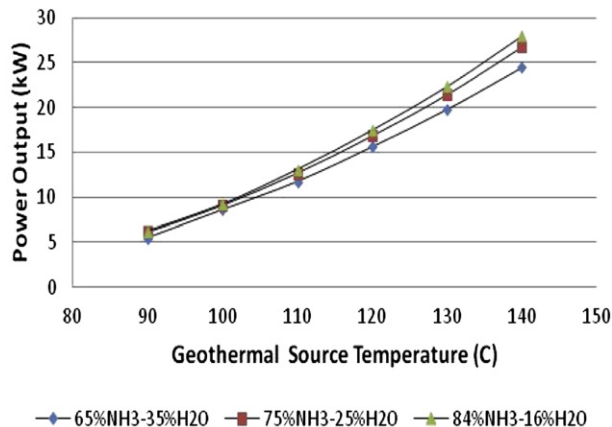


Fig. 14. Power output for the different composition of the working fluid.

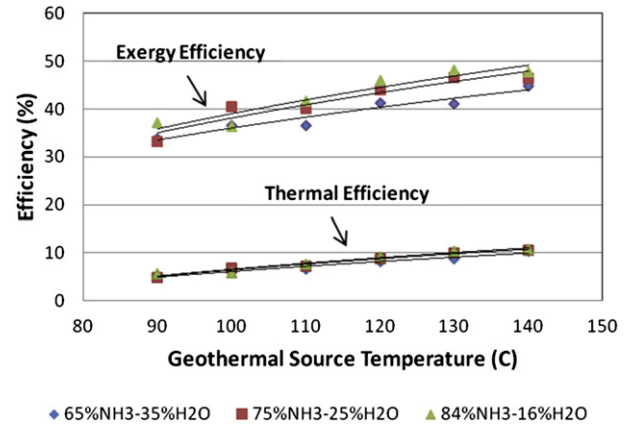


Fig. 15. Thermal and exergetic efficiency for the different composition of the working fluid.

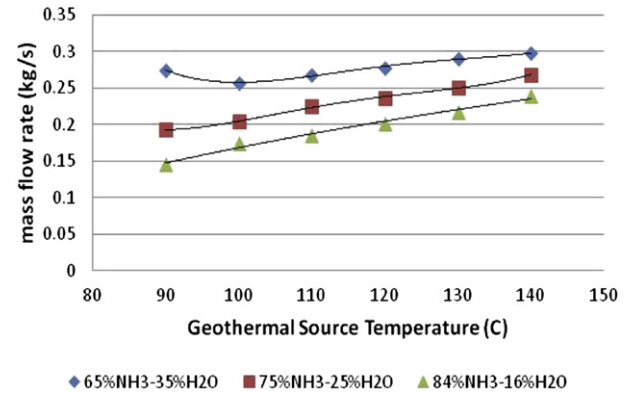


Fig. 16. Mass flow rate for the different composition of the working fluid.

$$q = \bar{U}A\Delta T_m = \bar{U}A \left[\frac{(T_{h1} - T_{c2}) - (T_{h2} - T_{c1})}{\ln[(T_{h1} - T_{c2})/(T_{h2} - T_{c1})]} \right] \quad (20)$$

The determination of the overall heat transfer coefficient (\bar{U}) is often tedious and needs data not available data at the preliminary stages of the design. As a first approximation, for preliminary calculations, the values shown below were

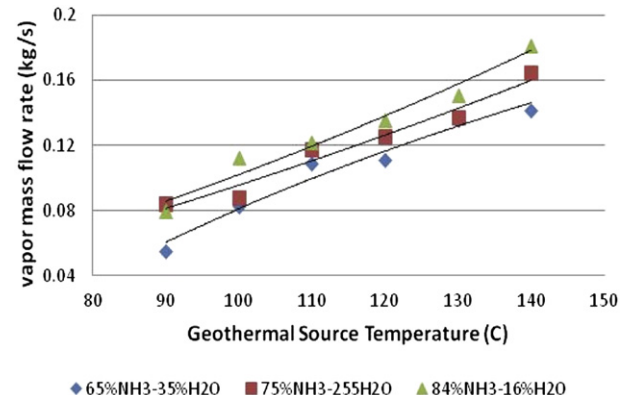


Fig. 17. Vapor mass flow rate for the different composition of the working fluid.

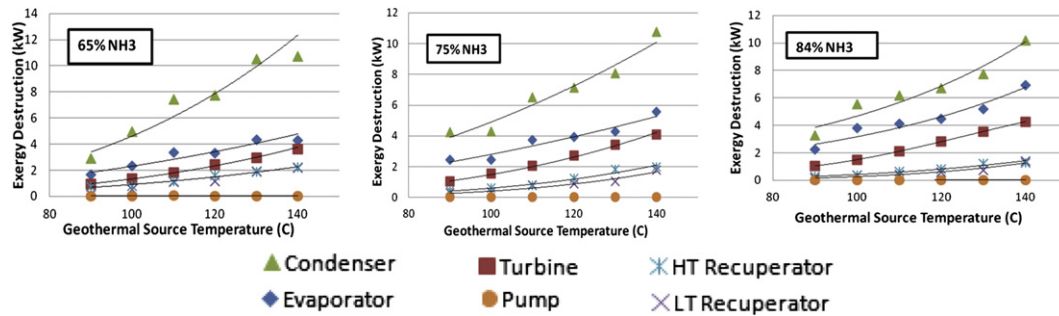


Fig. 18. Exergy destruction in the components of the Kalina cycle.

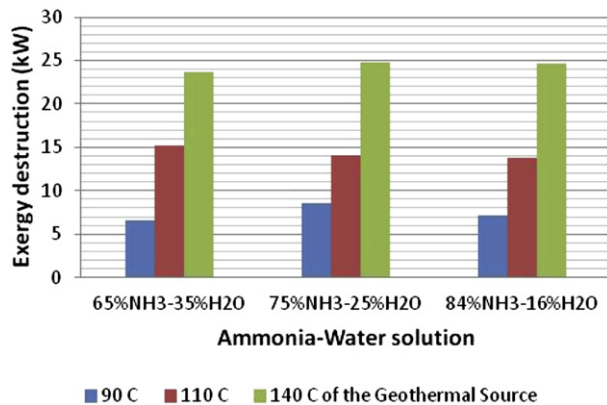


Fig. 19. Total exergy destruction for different composition of the working fluids in the Kalina cycle.

Table 3
Approximate values of \bar{U} for several situations.

Fluids	Overall heat transfer coefficient, \bar{U} W/m ² K
Ammonia–water (recuperator)–ammonia–water	1000
Ammonia–water (condensing)–water	1100
Ammonia–water (evaporating)–water	900
Propane, Butane or pentane (condensing)–water	730
Refrigerant (condensing)–water	650
Refrigerant (evaporating)–water	510

Table 4
Operational parameters of the EGS project for different energy conversion systems.

Operation parameters	ORC	Kalina cycle
Working fluid	R-290	84%NH ₃ –16%H ₂ O
Power output (kW)	1800	1848
Evaporator heat consumption (kW)	17027.78	29333.89
Circulation pump (kW)	356	92
Thermal efficiency (%)	8.47	6
Exergetic efficiency (%)	47.6	36.5
Evaporation pressure (kPa)	2797	2500
Condensation pressure (kPa)	1350	1200
Mass flow rate (kg/s)	54.93	34.75
Vapor mass flow rate (kg/s)	54.93	22.45
Cooling water temperature (°C)	25	25
Turbine efficiency (%)	85	85
Pump efficiency (%)	80	80

Table 5
EGS plant for power production.

Reservoir	ORC	Kalina cycle
Well (km)	3	3
Temperature C	100	100
Useful life (a)	30	30
<i>Geothermal fluid cycle</i>		
Geothermal fluid flow rate (m ³ /h)	720	720
Distance between wells (m)	500	500
<i>Binary plant unit</i>		
Working fluid flow rate (kg/s)	54.93	34.75
Installed capacity (MW)	1.8	1.848
Full load hours (h/year)	8000	8000
Auxiliary power need relating to installed capacity (%)	10	10

used. Since the heat exchangers can be built according to various geometrical designs, there are correction factors that must be used with the Equation (20) depending on the configuration [28].

The values of \bar{U} should be determined experimentally for the fluids to be used in the plant. As a first approximation for preliminary calculations, the values shown in Table 3 may be used [1,26–29].

The calculation of the binary plants unit costs was made based on past purchase orders, and quotations from experienced professional cost estimators [26,30]. For the heat exchangers, the costs calculation was based on the heat transfer areas while for the pump and turbine was based on the consumed and generated power respectively. The results are shown in Table 6.

ORC and Kalina cycle power production technology were assumed to be compared in the same EGS site. The reservoir is assessed with a deep well of a depth of 3000 m with three wells, (one injection and two production wells). The reservoirs are engineered with the same technical effort. The geothermal fluid is recovered from the reservoirs using submersible pumps in the production wells. The necessary data to define both plants are summarized in Table 5.

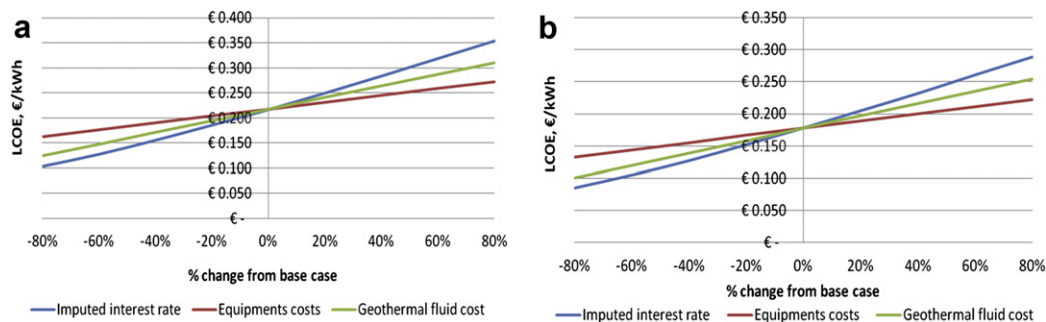
In order to verify the sensitivity of the levelized electricity costs on some economics parameters, such as: geothermal fluid cost, equipments costs and interest rate, it was elaborated a sensitivity graphs for the two different technologies, as shown in Fig. 20a and b.

The sensitivity analysis was performed ranging from –80% to 80% of the base case parameter. The parameter that most affects the cost per kW h is the interest rate, followed by the cost of the geothermal fluid. Government actions to promote this technology in conjunction with the development of the learning curve costs could lead this technology to values lower than 0.10 €/kW h.

Table 6

Cost and economic data of the defined EGS, using binary plants.

Economic data	ORC	Kalina cycle	Comment
Well cost	€ 9,000,000.00	€ 9,000,000.00	€3 million per well (1 injector, 2 producer)
Reservoir engineering	€ 2,250,000.00	€ 2,250,000.00	€0.75 million per well
Download pump	€ 1,440,000.00	€ 1,440,000.00	€2000 (m ³ /h)
Geothermal fluid loop	€ 250,000.00	€ 250,000.00	€500 per meters
Binary Plant unit (components + 10% pipping)	€ 1,702,425.10	€ 1,653,982.10	
Interconnections costs	€ 510,727.53	€ 496,194.63	30% plant costs
Civil works	€ 510,727.53	€ 496,194.63	30% plant costs
Installation of Plant Equipments	€ 595,848.79	€ 578,893.74	35% plant costs
Other costs	€ 1,625,972.89	€ 1,616,526.51	10% of total investments
Operating cost per year			
Personnel and consumables	€ 50,000.00	€ 50,000.00	Five operators
O&M subsurface	€ 168,750.00	€ 168,750.00	1.5% of subsurface investments (well doublet and reservoir engineering)
O&M surface	€ 203,545.51	€ 200,638.93	6% of surface investments (binary plant + geothermal fluid loop + downhole pump)
Annualized costs			
Imputed interest rate	11.5%	11.5%	
Economic lifetime	30	30	
Annualized investments (equipments)	€ 793,391.69	€ 780,967.76	
Annualized investments (well)	€ 1,345,096.08	€ 1,345,096.08	€/year
Total annualized investments	€ 2,138,487.77	€ 2,126,063.84	€/year
Annual operating costs	€ 2,510,783.28	€ 2,495,452.76	€/year
Electricity generated	11,552,000.0	14,048,000	kW h/year
LCOE	€ 0.217	€ 0.178	€/kW h

**Fig. 20.** Sensitivity analysis of EGS LCOE. a) ORC and b) Kalina cycle.

8. Conclusions

ORCs and Kalina cycles for geothermal power plants applications in the frame of low temperatures levels were investigated, so as to compare their thermodynamic and economic performance. On the basis of the calculations performed and with the assumptions considered, it emerges that:

1. There is an optimal working fluid for each geothermal source temperature. In the case of 100 °C, the best performance was obtained for R-290 fluid in the case of ORC. For Kalina cycle, the best performance was obtained with a composition of 84% of ammonia mass fraction and 16% of water mass fraction in the mixture. For these working fluids, Kalina cycle offer 18% more net power than ORC and require 37% less mass flow rate of working fluid.
2. It was obtained 17.8% lower levelized electricity costs for Kalina cycle over the ORC for an EGS working at 100 °C and 200 kg/s.
3. The actual costs of €/kW h, make this technology uneconomic, but this are set to fall in 10–15 year, making this technology competitive with most hydrocarbons if is added a carbon tax or carbon capture and storage facility and government incentives for cleans technologies.

As a conclusion it can be said that the adoption of the Kalina cycle may be reasonable in the geothermal power plants, because the low temperature of the source permit a gain in performance of the Kalina cycle with respect to ORC. Otherwise the final decision may be affected by the fact that Kalina cycle has a more complicated plant scheme and that is not yet a proven technology because there are a few commercial power plants so far.

Acknowledgements

The authors want to thanks the Coordination of Improvement of Higher Education (CAPES), The National Council of Technological and Scientific Development (CNPq) and The Foundation for Research Support of Minas Gerais State (FAPEMIG) for their collaboration and financial support in the development of the research work. Also want to thanks AES Tietê Company for funding the Project: "Technological Alternatives for the Implantation of Hybrid Geothermal Energy in Brazil from Low-Temperature Sources".

References

- [1] R. DiPippo, Geothermal Power Plants: Principles, Applications, Case Studies and Environmental Impact, second ed., Butterworth-Heinemann, 30 Corporate Drive, Suite 400, Burlington, MA 01803, 2008.

- [2] An assessment by an MIT-led interdisciplinary panel, The Future of Geothermal Energy, In: Impact of Enhanced Geothermal Systems (EGS) on the United States in the 21st Century, Massachusetts Institute of Technology, 2006, ISBN 0-615-13438-6.
- [3] T.C. Hung, T.Y. Shai, S.K. Wang, A review of organic Rankine cycles (ORCs) for the recovery of low-grade waste heat, *Energy* 22 (7) (1997) 661–667.
- [4] T.C. Hung, S.K. Wang, C.H. Kuo, B.S. Pei, K.F. Tsai, A study of organic working fluids on system efficiency of an ORC using low-grade energy sources, *Energy* 35 (2010) 1403–1411.
- [5] C.E.C. Rodríguez, C.A.R. Sotomonte, O.J. Venturini, E.E.S. Lora, Análise paramétrica de fluidos de trabalho utilizando Ciclo Orgânico de Rankine a partir de fontes geotérmicas de baixas temperaturas, CBtermo, Salvador de Bahia – Brasil, 2011.
- [6] B.F. Tchanche, G. Papadakis, G. Lambrinos, A. Frangoudakis, Fluid selection for a low temperature solar organic Rankine cycle, *Applied Thermal Engineering* 29 (2009) 2468–2476.
- [7] Y. Dai, J. Wang, L. Gao, Parametric optimization and comparative study of organic Rankine cycle (ORC) for low grade waste heat recovery, *Energy Conversion and Management* 50 (2009) 576–582.
- [8] H. Chen, G.D. Yogi, E.K. Stefanakos, A review of thermodynamic cycles and working fluids for the conversion of low-grade heat, *Renewable and Sustainable Energy Reviews* 14 (2010) 3059–3067.
- [9] I. Kalina, Combined cycle system with novel bottoming cycle, *ASME Journal of Engineering for Gas Turbine and Power* 106 (1984). 737 e 742A.
- [10] P. Roy, M. Désilets, N. Galanis, H. Nesreddine, E. Cayer, Thermodynamic analysis of a power cycle using a low-temperature source and a binary $\text{NH}_3\text{--H}_2\text{O}$ mixture as working fluid, *International Journal of Thermal Sciences* 49 (2000) 48–58.
- [11] P.K. Nag, A.V.S.S.K.S. Gupta, Exergy analysis of the Kalina cycle, *Applied Thermal Engineering* 18 (6) (1998) 427–439.
- [12] E. Thorin, (2000), Power cycles with ammonia–water mixture as working fluid, Analysis of different applications and the influence of thermophysical properties, Doctoral thesis, Department of Chemical Engineering and Technology, Energy Processes, Royal Institute of Technology, Stockholm, Sweden.
- [13] L.T. Bo, C.H. Kuo, W.C. Chi, Effect of working fluids on organic Rankine cycle for waste heat recovery, *Energy* 29 (2004) 1207–1217.
- [14] J.W. Lund, D.H. Freeston, T.L. Boyd, Direct utilization of geothermal energy 2010 worldwide review, in: *World Geothermal Congress 2010* (2010).
- [15] A.I. Papadopoulos, M. Stijepovic, P. Linke, On the systematic design and selection of optimal working fluids for organic Rankine cycles, *Applied Thermal Engineering* 30 (2010) 760–769.
- [16] P.J. Mago, L.M. Chamra, K. Srinivasan, C. Somayaji, An examination of regenerative organic Rankine cycles using dry fluids, *Applied Thermal Engineering* 28 (2008) 998–1007.
- [17] V. Maizza, A. Maizza, Unconventional working fluids in organic Rankine cycle for waste energy recovery systems, *Applied Thermal Engineering* 21 (2001) 381–390.
- [18] R. DiPippo, Second law assessment of binary plants generating power from low-temperature geothermal fluids, *Geothermics* 33 (2004) 565–568.
- [19] M. Mirolli, H. Hjartarson, H.A. Mlack, M. Ralph, Testing and operating experience of the 2 MW Kalina cycle geothermal power plant in Húsavík, Iceland, *OMMI* 1 (2) (2002).
- [20] R. Stryjek, J.H. Vera, PRSV: an improved Peng–Robinson equation of state for pure compounds and mixtures, *The Canadian Journal of Chemical Engineering* 64 (1986) 323–333.
- [21] B. Saleh, G. Koglbauer, M. Wendland, J. Fische, Working fluids for low-temperature organic Rankine cycles, *Energy* 32 (2007) 1210–1221.
- [22] M.S. Peters, K.D. Timmerhaus, in: *Plant Design and Economics for Chemical Engineers*, fourth ed., McGraw-Hill, New York, United States, 1991.
- [23] A. Bejan, G. Tsatsaronis, Moran, in: *M Thermal Design and Optimization*, John Wiley & Sons, New York, United States, 1995.
- [24] E. Huenges, *Geothermal Energy Systems*, In: Exploration, Development and Utilization, WILEY-VCH Verlag GmbH & Co. KGaA, Weinheim, Germany, 2010, ISBN 978-3-527-40831-3.
- [25] J.P. Holman, *Heat transfer*, McGraw-Hill Companies, 2002, p. 665.
- [26] P. Dorj, Thermoeconomic Analysis of a New Geothermal Utilization CHP Plant in Tsetserleg, Mongolia, MSc thesis, Department of Mechanical and Industrial Engineering, University of Iceland, ISBN 9979-68-166-7, 2005.
- [27] R. DiPippo, *Geothermal Power Plants: Principles, Applications and Case Studies*, Elsevier, Oxford UK, 2005, p. 183 (Chapter 8).
- [28] F.P. Incropera, D.P. DeWitt, *Fundamentals of Heat and Mass Transfer*, fourth ed., John Wiley & Sons, New York, 1996.
- [29] K.J. DiGenova, Design of organic Rankine cycles for conversion of waste heat in a polygeneration plant, Master of Science in Mechanical Engineering at the Massachusetts Institute of Technology, September 2011.
- [30] C.E.C. Rodríguez, J.C.E. Palacios, C.A.R. Sotomonte, O.J. Venturini, E.E.S. Lora, V.M. Cobas, D.M. Dos Santos, F.R.L. Dotto, V. Gialluca, Exergetic and Economic Analysis of Kalina Cycle for Low Temperature Geothermal Sources in Brazil, ECOS, Perugia, Italia, 2012.
- [31] P. Hearps, D. McConnell, *Renewable Energy Technology Cost Review*, In: Technical Paper Series, Melbourne Energy Institute, May 2011.
- [32] K. Ahmed, *Renewable Energy Technologies – A Review of the Status and Costs of Selected Technologies*, Technical Report No. 240, World Bank Technical Paper, Washington, 1994.
- [33] E. Huenges, *Geothermal Energy Systems*, In: Exploration, Development and Utilization, WILEY-VCH Verlag GmbH & Co. KGaA, Weinheim, 2010, ISBN 978-3-527-40831-3.
- [34] *Renewable Energy World Magazine* 14 (4) (July–August 2011). 2011–2012 Review Issue Plus Directory of Suppliers.
- [35] V.M. Hamza, R.R. Cardoso, A.J.L. Gomes, C.H. Alexandrino, Brazil: Country Update, in: *Proceedings World Geothermal Congress*, 2010.
- [36] A.A. Lakew, O. Bolland, Working fluids for low-temperature heat source, *Applied Thermal Engineering* 30 (2010) 1262–1268.